

Enthalpy and Heat Capacity of Solid Uranium Dioxide

Summary and Recommended Equations

Recommended equations for the enthalpy and heat capacity of solid UO_2 are based on a combined analysis of the available enthalpy data [1-6] from 483 to 3100 K, the heat capacity data from 293 to 1006 K [7-8] and the heat capacity data from 1997-2873 K from recent measurements by Ronchi et al.[9]. Heat capacity data reported by Affortit and Marcon [10], Affortit [11], Popov et al.[12] and Engel [13] were not included in the combined fit because they disagreed with the consensus and showed systematic errors. Although the λ -phase transition at 2670 K has been confirmed by high-temperature neutron diffraction and scattering experiments reported by Hutchings et al. [14-15] and by thermal analysis of UO_{2+x} cooling curves from 2300 to 3000 K by Hiernaut et al. [16], single equations for the enthalpy and heat capacity are recommended from 298 to 3120 K to provide the best fit to the high-temperature heat capacity data of Ronchi et al. Heat capacity data above and below the λ -phase transition show similar temperature behavior. The best fit to the enthalpy data was obtained with the equation:

for $298.15 \text{ K} \leq T \leq 3120 \text{ K}$

$$\begin{aligned}
 H(T) - H(298.15 \text{ K}) = & C_1 \theta \left[(e^{\theta/T} - 1)^{-1} - (e^{\theta/298.15} - 1)^{-1} \right] \\
 & + C_2 \left[T^2 - (298.15)^2 \right] \\
 & + C_3 e^{-E_d/T}
 \end{aligned} \tag{1}$$

where $C_1 = 81.613$,

$\theta = 548.68$,

$C_2 = 2.285 \times 10^{-3}$,

$C_3 = 2.360 \times 10^7$,

$E_d = 18531.7$,

T is the temperature in K and the enthalpy increment, $H(T) - H(298.15 \text{ K})$, is in $\text{J} \cdot \text{mol}^{-1}$.

The temperature derivative of Eq.(1) gives the heat capacity, C_p , in $\text{J} \cdot \text{mol}^{-1} \cdot \text{K}^{-1}$:

For $298.15 \text{ K} \leq T \leq 3120 \text{ K}$

$$C_p = \frac{C_1 \theta^2 e^{\theta/T}}{T^2 (e^{\theta/T} - 1)^2} + 2C_2 T + \frac{C_3 E_a e^{-E_a/T}}{T^2} \quad (2)$$

where the constants are identical to those for Eq.(1). The enthalpy data were fit about as well with the 7-term polynomial:

for $298.15 \text{ K} \leq T \leq 3120 \text{ K}$

$$\begin{aligned} H(T) - H(298.15 \text{ K}) = & - 21.1762 + 52.1743 \tau + 43.9753 \tau^2 \\ & - 28.0804 \tau^3 + 7.88552 \tau^4 - 0.52668 \tau^5 \\ & + 0.71391 \tau^{-1} \end{aligned} \quad (3)$$

where $\tau = T/1000$, T is the temperature in K, and the enthalpy increment, $H(T) - H(298.15 \text{ K})$, is in $\text{kJ} \cdot \text{mol}^{-1}$. The corresponding heat capacities were calculated from the temperature derivative of Eq.(3), which is:

for $298.15 \text{ K} \leq T \leq 3120 \text{ K}$

$$\begin{aligned} C_p(T) = & + 52.1743 + 87.951 \tau - 84.2411 \tau^2 \\ & + 31.542 \tau^3 - 2.6334 \tau^4 - 0.71391 \tau^{-2} \end{aligned} \quad (4)$$

where $\tau = T/1000$, T is the temperature in K, and the heat capacity, C_p , is in $\text{J} \cdot \text{mol}^{-1} \cdot \text{K}^{-1}$.

The enthalpy values from these two fits agree within 0.5% and cannot be distinguished in the graph in Figure 1, which compares these fits with the enthalpy data. Figure 2, which compares the heat capacity data with values calculated from Eq.(2) and Eq.(4), shows that the values obtained from these two equations are almost identical. They deviate by at most 1%, which is less than the scatter in the data. The λ -phase transition at 2670 K has been included in Figure 2. Because the fits

by both functional forms are almost identical both equations are recommended. However, because the individual terms of Eq.(1-2) are not related to the contributions from the physical processes, which can now be calculated from first principles [17, 18] and because polynomial forms are simpler for inclusion in large computer codes that are used in reactor-safety calculations, the polynomials given in Eqs.(3-4) may be preferred. Recommended values of the enthalpy and heat capacity calculated from Eqs.(1) and (2) are tabulated as a function of temperature in Table 1. Values calculated using the polynomial equations, Eq.(3) and Eq.(4), are tabulated in Table 2. Table 3 gives values per kg of UO_2 obtained from Eqs.(1) and (2). Table 4 gives values per kg of UO_2 obtained from the polynomial equations, Eq.(3) and Eq.(4).

Uncertainties

The uncertainty in the recommended enthalpy increments is $\pm 2\%$ from 298.15 K to 1800 K and $\pm 3\%$ from 1800 K to the melting point (3120K). The heat capacity uncertainty is $\pm 2\%$ from 298.15 to 1800 K; $\pm 13\%$ from 1800 to 3120 K. These uncertainties, shown in Figure 2, are based on the scatter in the data and the percent deviations of the data from the recommended equations. Because no attempt has been made to calculate the heat capacity peak in the vicinity of the λ -phase transition, as was done in the detailed analysis by Ronchi and Hyland [17], the heat capacity equation and uncertainties are not valid for temperatures close to the phase transition.

Discussion

Background and Theory

The existence of the λ -phase transition in solid UO_2 at 2670 K, that had been suggested by Bredig [19] and included in the enthalpy equations recommended by Fink [20, 21] and of Harding et al.[22] has been confirmed by Hutchings et al. [14-15] using neutron scattering experiments to study the oxygen defects and by Hiernaut et al. [16] from the analysis of cooling curves of UO_{2+x} . Hiernaut et al. [16] reported a λ -phase transition at 2670 ± 30 K in $\text{UO}_{2.00}$ and developed a model for the transition as a function of stoichiometry and temperature.

High-temperature neutron diffraction and inelastic scattering experiments on UO_2 and ThO_2 at temperatures from 293 to 2930 K reported by Hutchings et al. [14-15] provide direct evidence for thermally induced Frenkel oxygen lattice disorder at temperatures above 2000 K. The disorder has been identified as dynamic Frenkel type similar to that in halide fluorites with a Frenkel pair formation energy of 4.6 ± 0.5 eV. Hutchings [15] suggests that the high oxygen vacancy concentrations and their mobility at high temperatures may be related to the observed high creep rate [23] and softening or plasticity of UO_2 above 2500 K. He also reported that inelastic magnetic scattering on lowest magnetic energy levels of U^{4+} indicate that excitation of these levels make a significant contribution to the heat capacity in UO_2 .

Hiernaut et al. [16] determined that the transition temperature in nominally stoichiometric $\text{UO}_{2.00}$ is at 2670 ± 30 K, which is coincident with the transition temperature proposed by Bredig [19] but higher than the 2610 K value proposed by Ralph and Hyland [24]. The scatter in the data of Hiernaut et al. was approximately twice the precision of the temperature measurement. The transition was identified as a first-order phase transition from cooling curves in the temperature range of 2300 to 3000 K. The transition temperature for substoichiometric urania (UO_{2-x}) increased with increasing x (i.e. reduction of the sample in a 3% hydrogen atmosphere) and the cooling curves exhibit undercooling indicative of a first-order transition. No transition was detected in UO_{2+x} .

Heirnaut et al.[16] found that the phase transition in stoichiometric $\text{UO}_{2.00}$ was consistent with that in stoichiometric non-actinide fluorites (e.g. SrCl_2), where the high-temperature phase is established rapidly but continuously. They modeled the λ -like phase transition in $\text{UO}_{2.00}$ as a second-order transition involving oxygen Frenkel disorder. Their model is consistent with the second-order λ -transition in $\text{UO}_{2.00}$ converting to a first-order phase transition in UO_{2-x} . Although no transition was detected in UO_{2+x} , their model is consistent with a second-order transition that decreases with increasing x from $T=2670$ K at $x=0$ to cross the U_4O_9 phase boundary near 973 K, where a diffuse order-disorder transition is observed in the U_4O_9 oxygen sublattice. They suggest that the second-order λ -transition in $\text{UO}_{2.00}$ is the stoichiometric counterpart of the interstitial superlattice transition in U_4O_9 . Heirnaut et al.[16] conclude that they did not detect a transition

in UO_{2+x} because the transition rapidly decreases in peak height and increases in peak width with x . Based on their experimental results and their model, they have modified the U-O phase diagram to include these transitions.

From interpretation of these experimental data, Ronchi and Hyland [17] calculated the contributions from each process to compare with available data and provided an excellent description of the theoretical understanding of the contributions from each physical process to the heat capacity. The dominant contributions in each of four temperature intervals for the solid discussed in detail by Ronchi and Hyland [17] are summarized below.

- (1) From room temperature to 1000 K, the increase heat capacity is governed by the harmonic lattice vibrations, which may be approximated by a Debye model. By 1000 K, this contribution becomes constant. A smaller contribution is provided by thermal excitation of localized electrons of U^{4+} ($5f$)² in the crystal field levels. This crystal field contribution is proportional to T at low temperatures but becomes temperature independent at high temperatures where the concentration of U^{4+} decreases as the concentrations of U^{3+} and U^{5+} increase.
- (2) From 1000 to 1500 K, the heat capacity increases due to increases in the anharmonicity of the lattice vibrations as evidenced in the thermal expansion. This contribution has been previously referred to as the thermal expansion or dilation contribution.
- (3) From 1500 to 2670 K, the increase in heat capacity is due to formation of lattice and electronic defects. The peak in the heat capacity at 2670 K (85.6% of the melting point) has been attributed to Frenkel defects both from theoretical considerations and neutron scattering measurements of the oxygen defect concentration as a function of temperature. A similar discontinuity and anion behavior was observed for ThO_2 [14,15]. Harding et al. [22] comment that because no excess enthalpy is evident in ThO_2 below the corresponding transition, it is reasonable to suggest that the increase in UO_2 below the phase transition is due to coupling between electronic disorder and Frenkel disorder. Ronchi and Hyland [17] point out that the increase in the electrical conductivity in this temperature interval indicates

a contribution from electronic defects but the small polaron contribution from electron-hole interactions is minor compared to contributions due to Frenkel defects.

- (4) Above the phase transition temperature, the peak of the heat capacity drops sharply due to rapid saturation of the defect concentration. From 2700 K to the melting point, Schottky defects become important.

Review and Analysis of Experimental Data

Recently, Ronchi et al. [9] made simultaneous measurements of the heat capacity and thermal diffusivity from 2000 to 2900 K. Although these measurements lacked the sensitivity required to detect the phase transition peak, they showed that above the λ -phase transition, the heat capacity has a temperature dependence that is similar to that prior to the phase transition. Figure 3 shows that the heat capacity data of Ronchi et al.[9] at temperatures higher than the λ -phase transition are inconsistent with the constant heat capacity that was recommended by Fink et al. [20, 21] and by Harding et al. [22], and with the theoretical calculation of Ronchi and Hyland [17]. The heat capacity equation in the MATPRO database [25], also shown in Figure 3, does not provide a good representation of these high-temperature data even though this equation gives heat capacity values that increase with temperature. Therefore, all available heat capacity and enthalpy data for solid UO_2 have been reviewed and a combined analysis of enthalpy and heat capacity data has been made to obtain equations for the enthalpy increments and heat capacities that are consistent with each other and with the experimental data.

Comparison of the available enthalpy data, shown in Figure 1, indicates that the data from 1174 to 3112 K of Hein and Flagella [3,4] are in good agreement with the data of Leibowitz, Mishler and Chasanov [1] from 2561 to 3088 K and with the data of Fredrickson and Chasanov [2] from 674 to 1436 K. Data given by Hein, Sjodahl and Szwarc [4] is identical to that reported by Hein and Flagella [3]. Data reported by Conway and Hein [26] in 1965 are preliminary results of the data published in 1968. Therefore, these preliminary data have not been included in this analysis. The 1947 measurements by Moore and Kelley [5] from 483 to 1464 K tend to be slightly high relative

to the data of Fredrickson and Chasanov [2]. The data of Ogard and Leary (from 1339 to 2306 K) [6] are consistently high relative to the data of Hein and Flagella [3] and that of Fredrickson and Chasanov [2].

Figure 4 shows all the available heat capacity data. The heat capacity data of Affortit and Marcon [10] and of Affortit [11], that are labeled “Affortit” in Figure 4, clearly disagree with other data. Therefore these data were not included in the combined analysis. The variances (square of the standard deviations) of these data from a smooth curve through all the data are 100 to 1000 times larger than variances of data included in the analysis. Figure 5, which shows the low-temperature heat capacity data, indicates that the heat capacity data from 5 to 346 K of Hunzicker and Westrum [7] and that of Gronvold et al. [8] (304-1006 K) are in good agreement in the temperature range of overlap. However, between 500 and 800 K, the data of Gronvold et al. [8] are high because of contamination of the sample by U_4O_9 . Data from 433 to 876 K of Popov et al. [12] were excluded from the combined analysis because they are consistently higher than the data of Gronvold et al. Figure 5 shows that the data of Engel [13] (300 to 1000 K) appear to have a systematic error because they differ from other data by a normalization. Thus the data of Engel have not been included in the combined analysis. The variances for the data of Popov et al. and that of Engel from a smoothed curve through all the data are about a factor of 20 higher than the variances for data included in this analysis.

A combined fit of the enthalpy and heat capacity data [1-9], which are listed in Table 5, has been made using a nonlinear weighted χ^2 minimization procedure. Data from each experiment was weighted by the inverse of the square of the standard deviation of that set of data from a smooth curve through all the data in that temperature range. The smooth curves used for the enthalpy data and the low-temperature heat capacity data were those defined by the polynomials of Harding et al. [21], which are identical with the values from the equations of Fink et al. [19,20]. For the two sets of data of Ronchi et al. [9], the standard deviations from the curve given by Ronchi et al. were used to determine appropriate weights. The temperatures of data obtained prior to 1969 were converted from the 1948 International Practical Temperature Scale (IPTS) to the 1968 IPTS.

The combined fits of the enthalpy and heat capacity data were constrained by:

$$H(T) - H(298.15\text{K}) = 0 \text{ at } 298.15 \text{ K and}$$

$$\left(\frac{\partial H}{\partial T}\right)_P = C_p$$

where $H(T) - H(298.15\text{K})$ is the enthalpy increment and C_p is the heat capacity. Some of the functional forms considered are listed in Table 6. Forms included polynomials as well as functional forms that approximated the physical processes that were shown to be important by the theoretical work of Ronchi and Hyland [17]. The lattice term, which was used in the equation of Kerrisk and Clifton [27] and in the low-temperature equation of Fink et al. [20,21], approximates the harmonic lattice contribution. The T^2 term accounts for the anharmonicity of the lattice as given by dilation. Both an exponential term, $C e^{-E/T}$, and a term with temperature times the exponential, $C T e^{-E/T}$, were considered for describing the contributions from defects. Frenkel defects are more appropriately described by the term $C e^{-E/T}$. The electronic small polaron contribution is better described by the functional form $C T e^{-E/T}$. The combined data were fit better using $C e^{-E/T}$ to describe the defect contribution, which is consistent with calculations by Ronchi and Hyland [17] that indicated that contributions to the heat capacity due to Frenkel defects are larger than the electronic small polaron contribution.

Browning et al. [18] have commented that the ability to calculate the magnitude of each contribution to the enthalpy from physical principles, as has been done by Ronchi and Hyland [17], makes analysis of the enthalpy data based on a least squares fitting procedure using approximate functional forms obsolete because the fitting procedure does not account for all physical processes and therefore gives values for parameters in each functional term that differ from the known physical values. For example, the Debye and Einstein temperatures of UO_2 are well known and different from the values obtained in such a fitting procedure. However, Browning et al. [18] concur that functional forms that approximate physical processes provide a better fit to the experimental data than do fits using polynomials. This combined least squares analysis showed that the combined enthalpy and heat capacity data could not be well fit by a polynomial using the χ^2 minimization procedure unless the first guess of the coefficients was very close to the final values. The recommended polynomial

equation was obtained by using a linear regression to obtain a polynomial approximation to closely spaced enthalpy increments calculated from Eq.(1) and using the terms of that polynomial as a first guess for the nonlinear least squares fit of the enthalpy and heat capacity data

Both single equations for the entire temperature range and two equations (one below and one above the transition at 2670 K) were considered. Table 6, which tabulates the values of the variances for the enthalpy data, the heat capacity data, and the combined enthalpy and heat capacity data for the functional forms evaluated, shows that the use of two equations did not improve the fit to the combined data. The reason for this is clear from examination of the fits to the high-temperature heat capacity data in Figure 6 and the enthalpy data in Figure 7. The linear heat capacity equation that is the best fit to the heat capacity data above 2670 K results in a quadratic equation for the enthalpy increments, which is high relative to the enthalpy data. The heat capacity increase above the λ -phase transition seems inconsistent with the enthalpy data above this transition, because the slope of the enthalpy data above 3000 K is less than the slope below the transition. Further enthalpy and heat capacity data are needed above the λ -phase transition to resolve this apparent inconsistency. Thus, the best fit to the combined data is a single equation that is a compromise between the best fit to the high-temperature enthalpy data and the best fit to the high-temperature heat capacity data.

Table 6 shows that the smallest total variance was obtained for the 7-term polynomial because it gives the best fit to the low-temperature heat capacity data, which have large weights and a large number of points. However, Eq.(1), containing lattice, T^2 , and exponential terms, fits most data sets better than the polynomial, as shown in Table 5. The variances shown in Table 6 indicate that the best fit to the enthalpy data was with Eq.(1). The enthalpy values from these two fits agree within 0.5% and cannot be distinguished in the graph in Figure 1. The closeness of these two fits to the enthalpy data is indicated by the percent deviations of the enthalpy data from each equation, which are plotted in Figure 8. The percent deviation is defined as:

$$\% \text{ Deviation} = \frac{(\text{Equation} - \text{Data})}{\text{Data}} 100\% \quad (5)$$

Figure 2, which compares the heat capacity data with values calculated from Eq.(2) and Eq.(4), shows that the values obtained from these two equations are almost identical. They deviate by at most 1%, which is less than the scatter in the data, as shown by the deviation plot in Figure 9. Because the fits by both functional forms are almost identical both equations are recommended. However, because the individual terms of Eq.(1-2) are not related to the contributions from the physical processes, which can now be calculated from first principles [17,18] and because polynomial forms are simpler for inclusion in large computer codes that are used in reactor-safety calculations, the polynomials given in Eqs.(3-4) may be preferred.

Comparison with Existing Equations

Previously recommended [28] equations developed by Fink et al.[20,21] and Harding et al.[22], which give a constant heat capacity above 2670 K are not consistent with the heat capacity data of Ronchi et al.[9] above 2670 K. Figure 10 shows that the MATPRO [25] single equation does not provide as good a fit to these data as the recommended equations.

References

1. L. Leibowitz, L. W. Mishler, and M. G. Chasanov, *J. Nucl. Mater.* **29**, 356 (1969).
2. D. R. Fredrickson and M. G. Chasanov, *J. Chem. Thermodynamics* **2**, 263 (1970).
3. R. A. Hein and P. N. Flagella, *Enthalpy Measurements of UO₂ and Tungsten to 3260 K*, GE Report GEMP-578, General Electric, February 16, 1968.
4. R. A. Hein, L. A. Sjodahl, and R. Szwarc, *J. Nucl. Mater.* **25**, 99 (1968).
5. G. E. Moore and K. K. Kelly, *J. Am. Chem. Soc.* **69**, 2105 (1947).
6. A. E. Ogard and J. A. Leary, *High-Temperature Heat Content and Heat Capacity of Uranium Dioxide and Uranium Dioxide-Plutonium Dioxide Solid Solutions*, in *Thermodynamics of Nuclear Materials 1967*, IAEA, Vienna, p. 651 (1969).
7. J. J. Hunzicker and E. F. Westrum, *J. Chem. Thermodynamics* **3**, 61 (1971).
8. F. Gronvold, N. J. Kvseth, A. Sveen, and J. Tichy', *J. Chem. Thermo.* **2**, 665 (1970).
9. C. Ronchi, M. Sheindlin, M. Musella, and G. J. Hyland, *J. Applied Phys.* **85**, 776-789 (1999).
10. C. Affortit and J. Marcon, *Rev. Int. Hautes Temp. et Refract.* **7**, 236 (1970).
11. C. Affortit, *High Temperatures-High Pressures* **1**, 27-33 (1969).
12. M. M. Popov, G. L. Galchenko, and M. D. Seniv, *Zh. Neorg. Kim.* **3**, 1734 (1958) [English translation of *J. Inorganic Chem USSR* **3**, 18 (1958)].
13. T. K. Engel, *J. Nucl. Mater.* **31**, 211 (1969).
14. M. T. Hutchings, *High-Temperature Studies of UO₂ and ThO₂ using Neutron Scattering Techniques*, *J. Chem. Soc. Faraday Trans. II* **83**, 1083-1103 (1987).
15. M. T. Hutchings, K. Clausen, M. H. Dicken, W. Hayes, J. K. Kjems, P. G. Schnabel, and C. Smith, *J. Phys. C* **17**, 3903 (1984).
16. J. P. Hiernaut, G. J. Hyland, and C. Ronchi, *Premelting Transition in Uranium Dioxide*, *Int. J. Thermophys.* **14**(2), 259-283 (1993).
17. C. Ronchi and G. J. Hyland, *Analysis of Recent Measurements of the Heat Capacity of*

- Uranium Dioxide*, J. of Alloys and Compounds **213/214**, 159-168 (1994).
18. P. Browning, G. J. Hyland, and J. Ralph, *The Origin of the Specific Heat Anomaly in Solid Urania*, High Temperatures-High Pressures **15**, 169-178 (1983).
 19. M. A. Bredig, *L'étude des Transformations Crystalline a Hautes Temperatures*, Proceedings of a Conference held in Odeillo, France, 1971 (CNRS, Paris, 1972), p. 183
 20. J. K. Fink, *Enthalpy and Heat Capacity of the Actinide Oxides*, Int. J. Thermophys. **3**(2), 165-200 (1982).
 21. J. K. Fink, M. G. Chasanov, and L. Leibowitz, *Thermophysical Properties of Uranium Dioxide*, J. Nucl. Mater. **102**, 17-25 (1981); also as ANL Report ANL-CEN-RSD-80-3, Argonne National Laboratory (April 1981).
 22. J. H. Harding, D. G. Martin, and P. E. Potter, *Thermophysical and Thermochemical Properties of Fast Reactor Materials*, Commission of the European Communities Report EUR 12402 EN (1989).
 23. L. Leibowitz, J. K. Fink, and O. D. Slagle, *Phase Transitions, Creep, and Fission Gas Behavior in Actinide Oxides*, J. Nucl. Mater. **116**, 324-325 (1983).
 24. J. Ralph and G. J. Hyland, *Empirical Confirmation of a Bredig Transition in UO_2* , J. Nucl. Mater. **132**, 76 (1985).
 25. D. T. Hagrman, editor, *SCADAP/RELAP5/MOD 3.1 Code Manual Vol. 4: MATPRO - a library of materials properties for light-water-reactor accident analysis*, NUREG/CR-6150 (1995).
 26. J. B. Conway and R. A. Hein, J. Nucl. Mater. **15**, 149 (1965).
 27. J. F. Kerrisk and D. G. Clifton, *Smoothed Values of the Enthalpy and Heat Capacity of UO_2* , Nucl. Technol. **16**, 531 (1972).
 28. J. K. Fink and M. C. Petri, *Thermophysical Properties of Uranium Dioxide*, Argonne National Laboratory Report ANL/RE-97/2 (February 1997)

**Table 1. Enthalpy and Heat Capacity of UO₂ per mole of UO₂
Calculated from Equations (1) and (2)**

Temperature K	Enthalpy H(T)-H(298.15 K) kJ/mol	Heat Capacity C_p J/(mol K)
298.15	0.00	63.4
300	0.12	63.6
400	6.93	71.8
500	14.3	76.2
600	22.1	78.9
700	30.1	80.8
800	38.2	82.1
900	46.5	83.2
1000	54.9	84.2
1100	63.3	85.0
1200	71.9	85.7
1300	80.5	86.5
1400	89.2	87.4
1500	98.0	88.4
1600	106.9	89.7
1700	115.9	91.5
1800	125.2	93.8
1900	134.7	96.8
2000	144.6	100.6
2100	154.9	105.3
2200	165.7	111.1
2300	177.1	117.9
2400	189.3	125.9
2500	202.3	134.9
2600	216.3	145.1
2700	231.4	156.4
2800	247.6	168.6
2900	265.2	181.9
3000	284.0	196.0
3100	304.4	210.9
3120	308.6	214.0

**Table 2. Enthalpy and Heat Capacity of UO₂ per mole of UO₂
Calculated from Polynomial Equations (3) and (4)**

Temperature K	Enthalpy H(T)-H(298.15 K) kJ/mol	Heat Capacity C_p J/(mol K)
298.15	0.00	63.7
300	0.12	63.9
400	6.91	71.4
500	14.3	76.0
600	22.1	79.1
700	30.1	81.2
800	38.3	82.6
900	46.6	83.5
1000	55.0	84.1
1100	63.4	84.5
1200	71.9	85.0
1300	80.4	85.5
1400	89.0	86.3
1500	97.7	87.4
1600	106.5	88.9
1700	115.5	91.0
1800	124.7	93.6
1900	134.2	97.0
2000	144.1	101.1
2100	154.5	106.1
2200	165.4	112.0
2300	176.9	118.8
2400	189.1	126.6
2500	202.2	135.4
2600	216.3	145.3
2700	231.3	156.3
2800	247.6	168.4
2900	265.1	181.7
3000	283.9	196.1
3100	304.3	211.7
3120	308.6	214.9

**Table 3. Enthalpy and Heat Capacity of UO₂ per kg of UO₂
Calculated from Equations (1) and (2)**

Temperature K	Enthalpy H(T)-H(298.15 K) kJ/kg	Heat Capacity Cp J/(kg K)
298.15	0.00	235
300	0.43	235
400	25.7	266
500	53.1	282
600	81.9	292
700	111	299
800	142	304
900	172	308
1000	203	312
1100	235	315
1200	266	318
1300	298	320
1400	330	324
1500	363	327
1600	396	332
1700	429	339
1800	464	347
1900	499	358
2000	535	373
2100	574	390
2200	614	411
2300	656	437
2400	701	466
2500	749	500
2600	801	537
2700	857	579
2800	917	625
2900	982	674
3000	1052	726
3100	1127	781
3120	1143	792

**Table 4. Enthalpy and Heat Capacity of UO₂ per kg of UO₂
Calculated from Polynomial Equations (3) and (4)**

Temperature K	Enthalpy H(T)-H(298.15 K) kJ/kg	Heat Capacity Cp J/(kg K)
298.15	0.00	236
300	0.44	237
400	25.6	264
500	53.0	281
600	81.7	293
700	111	301
800	142	306
900	173	309
1000	204	311
1100	235	313
1200	266	315
1300	298	317
1400	330	319
1500	362	324
1600	394	329
1700	428	337
1800	462	347
1900	497	359
2000	534	375
2100	572	393
2200	612	415
2300	655	440
2400	700	469
2500	749	501
2600	801	538
2700	857	579
2800	917	624
2900	982	673
3000	1052	726
3100	1127	784
3120	1143	796

Table 5 Percent standard deviations of data from the best combined fits of the enthalpy and heat capacity of solid UO₂

Data Reference	Temperature Range (K)	N	% Standard Deviations	
			Polynomial	Eq.(1-2)
Enthalpy				
Ogard & Leary 1968 [6]	1339-2306	13	3.04	2.25
Moore & Kelly 1947 [5]	483-1464	14	1.80	1.50
Fredrickson & Chasanov 1970 [2]	674-1436	24	0.73	0.62
Hein and Flagella 1968 [3,4]	1174-3112	33	0.90	0.86
Leibowitz et al. 1969 [1]	2561-3088	12	1.85	1.60
Heat Capacity				
Huntzicker & Westrum 1971 [7]	293-346	9	0.72	0.57
Gronvold et al. 1970 [8]	304-1006	88	0.64	0.77
Ronchi et al. 1999 [9]	1997-2873	54	5.96	4.58

N = number of data

$$\% \text{ Standard Deviation} = \left(\frac{\sum \left[\frac{(\text{Fit}-\text{Data})}{\text{Data}} 100\% \right]^2}{N-\text{free parameters}} \right)^{1/2}$$

Table 6 Variances, σ^2 , of weighted fits for different equation forms

Enthalpy Functional Form	# of Parameters	Total σ^2	H σ^2	$C_p \sigma^2$
Lattice +T ² + exponential, Eq.(1)	5	0.34	0.25	0.47
Polynomial, Eq.(3)	7	0.32	0.28	0.38
Lattice +T ² +T exponential	5	0.55	0.40	0.73
T<2670 K: Lattice+T ² +exponential T>2670K: Quadratic	8	0.36	0.31	0.38
T<2670 K: Lattice+T ² +exponential T>2670K, quadratic+exponential	10	0.35	0.29	0.45

$$\sigma^2 = \frac{\frac{1}{N - \text{free}} \sum \frac{1}{\sigma_i^2} [y_i - y(T_i)]^2}{\frac{1}{N} \sum \frac{1}{\sigma_i^2}}$$

where N= number of data, free = # of free parameters, $(1/\sigma_i)^2$ = weight,
 y_i = datum, $y(T_i)$ = fit at temperature T_i

$$\text{Lattice} = \frac{C_1 \theta}{(e^{\theta/T} - 1)}$$

where C_1 and θ are parameters.

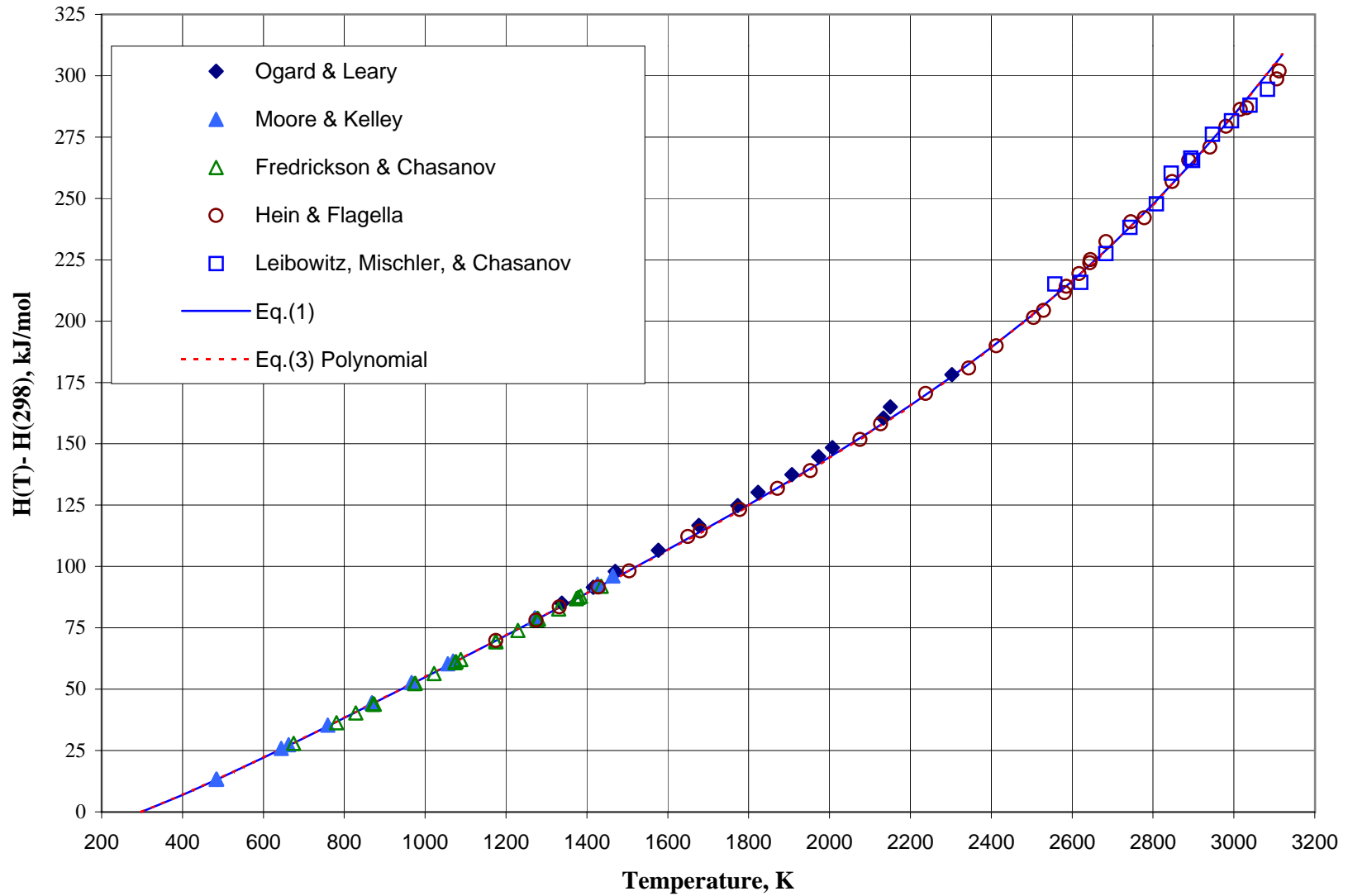
Figure 1 Enthalpy of Solid UO_2 

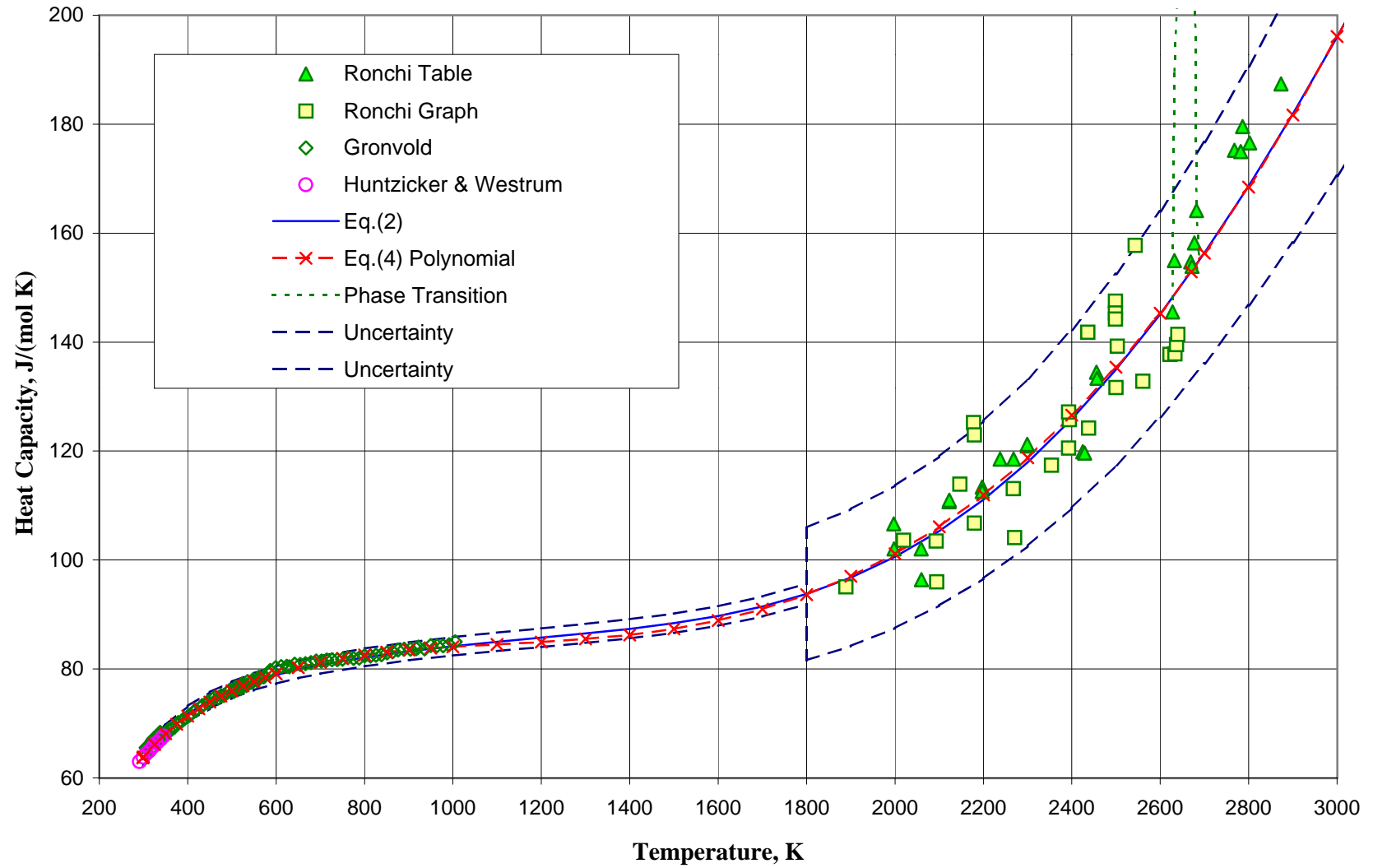
Figure 2 Heat Capacity of UO_2 

Figure 3 UO₂ Heat Capacity Data of Ronchi et al. Compared with Equations

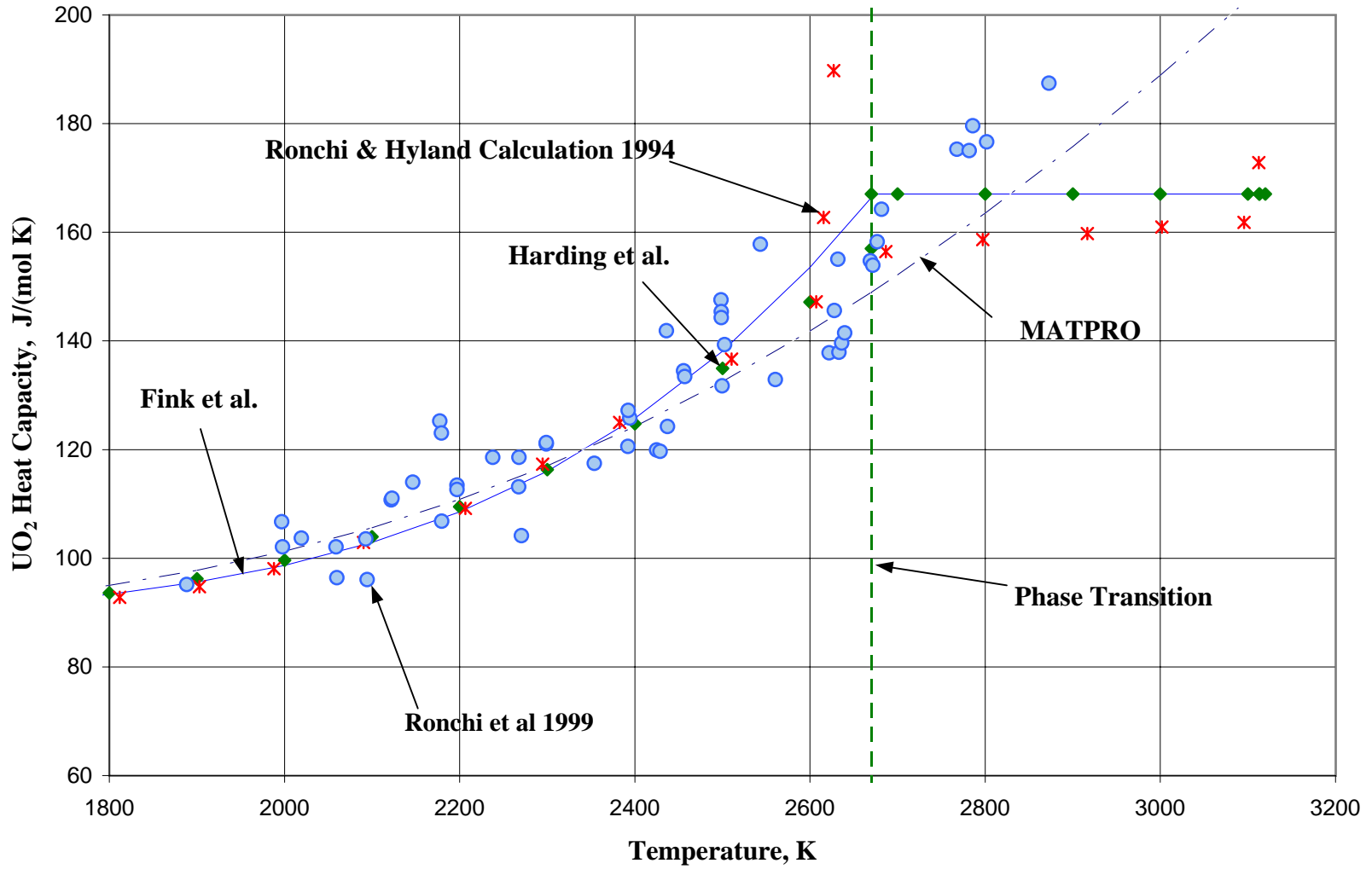


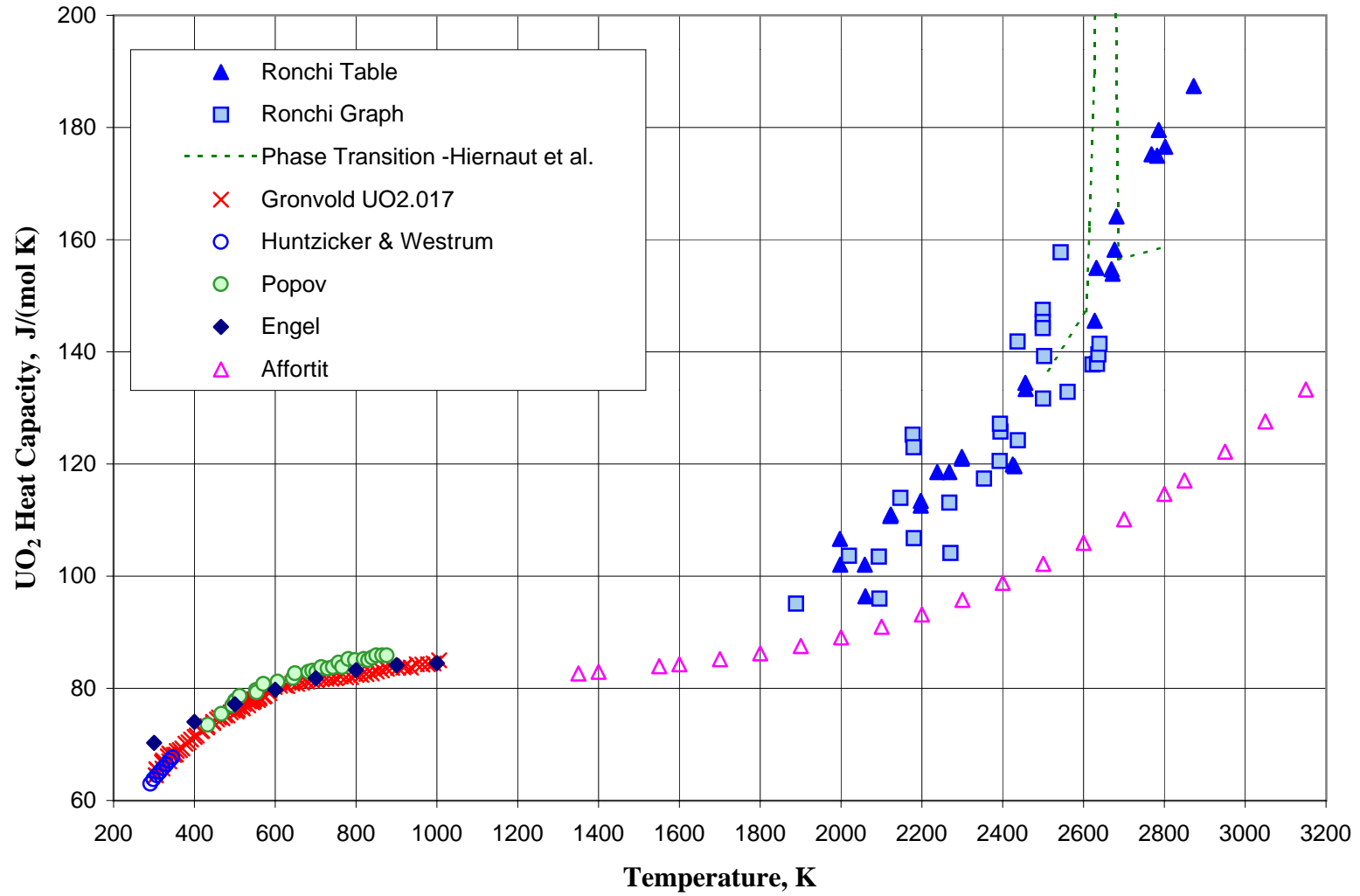
Figure 4 Solid UO₂ Heat Capacity Data

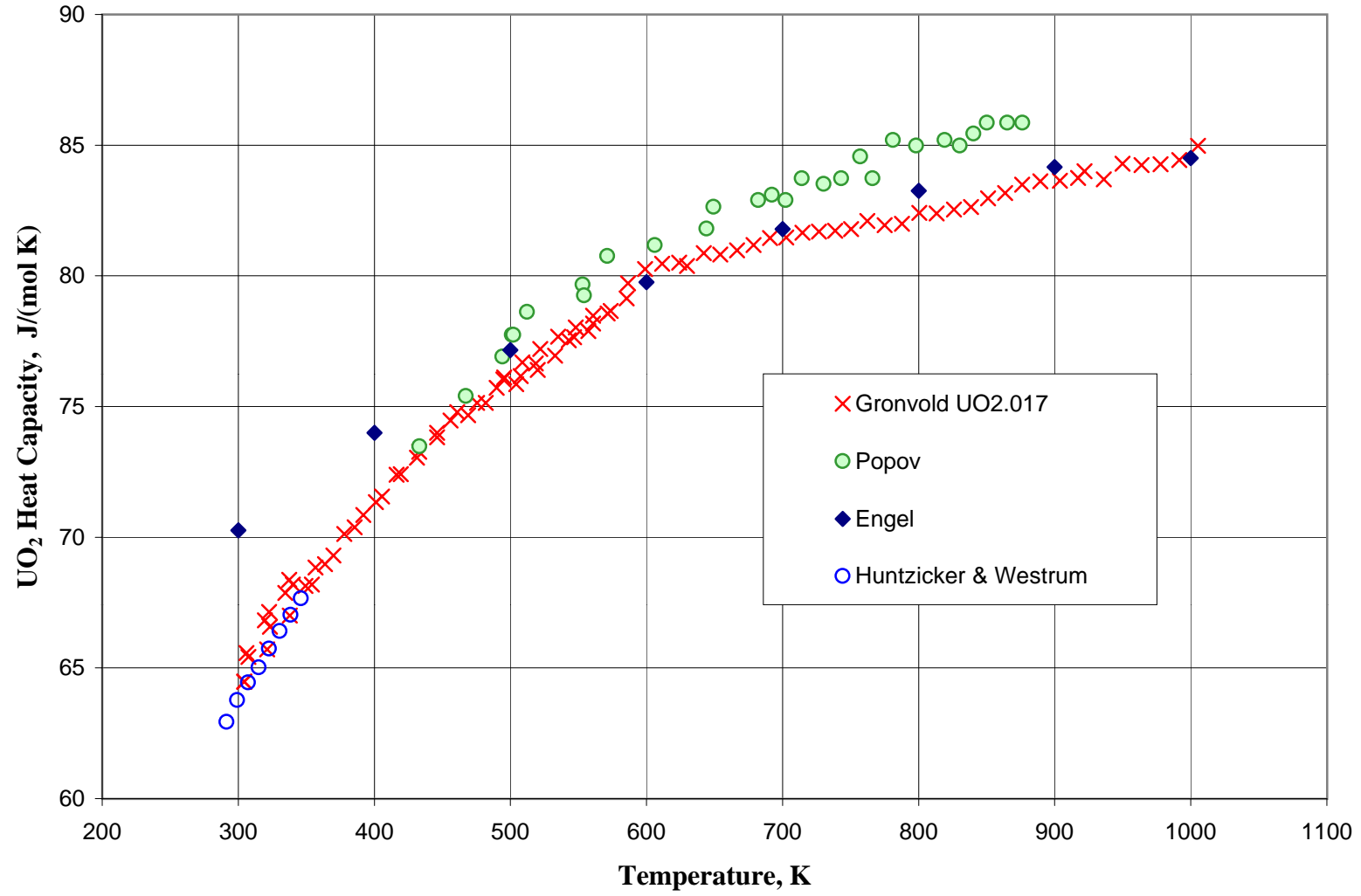
Figure 5 Low Temperature Solid UO₂ Heat Capacity Data

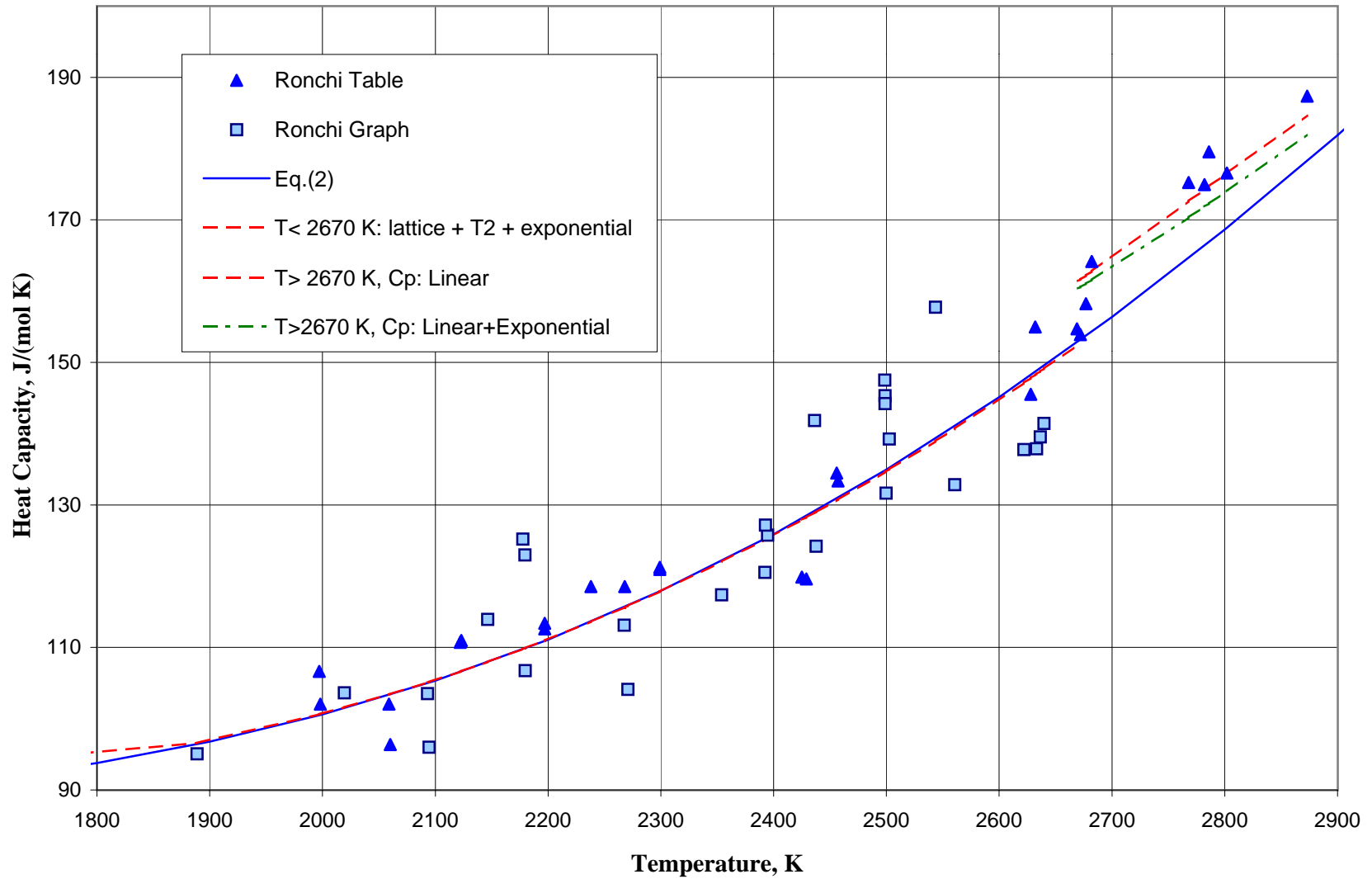
Figure 6 UO₂ Heat Capacity Forms With & Without Break at 2670 K

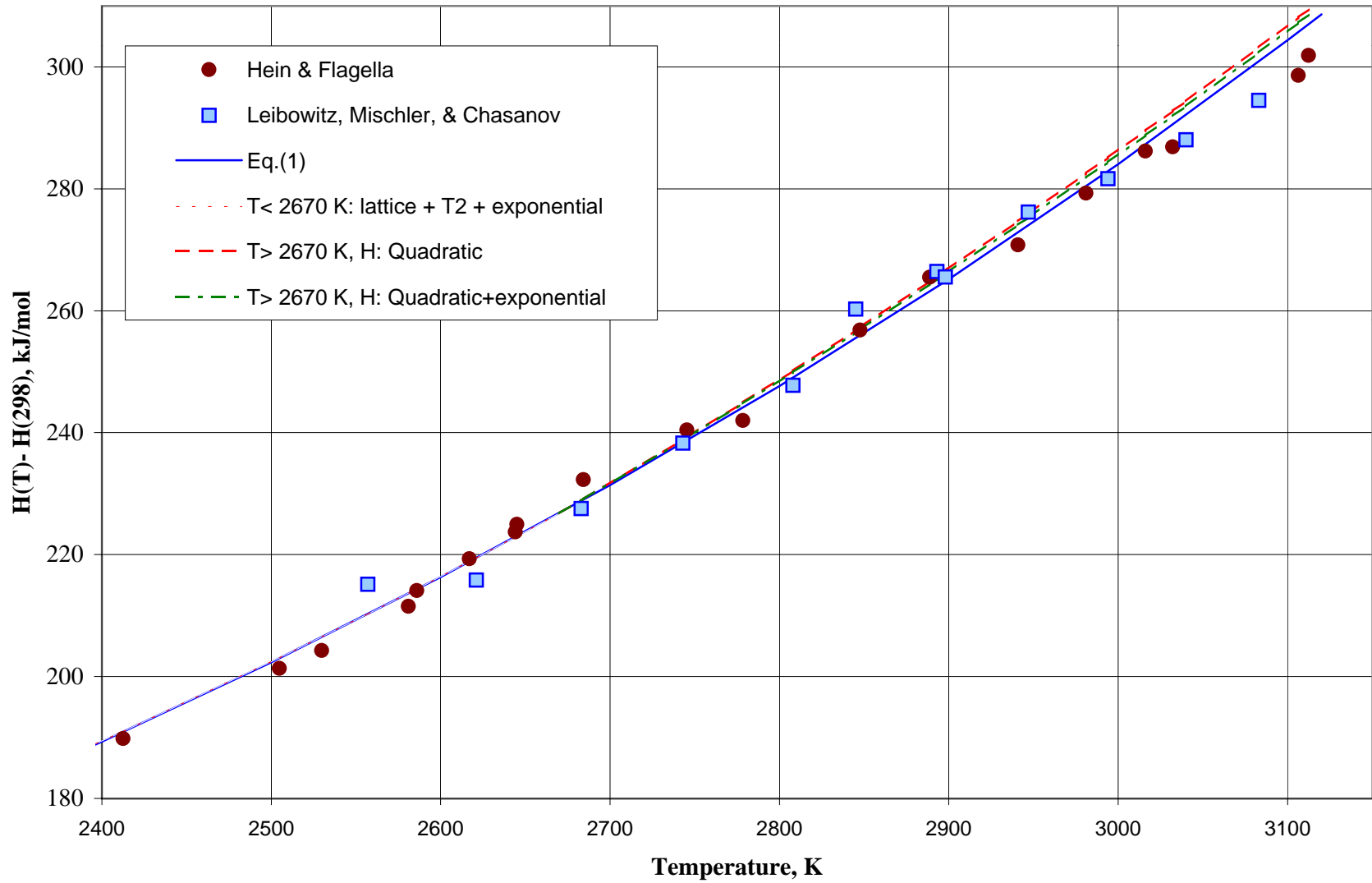
Figure 7 UO₂ Enthalpy Equations With and Without Break at 2670 K

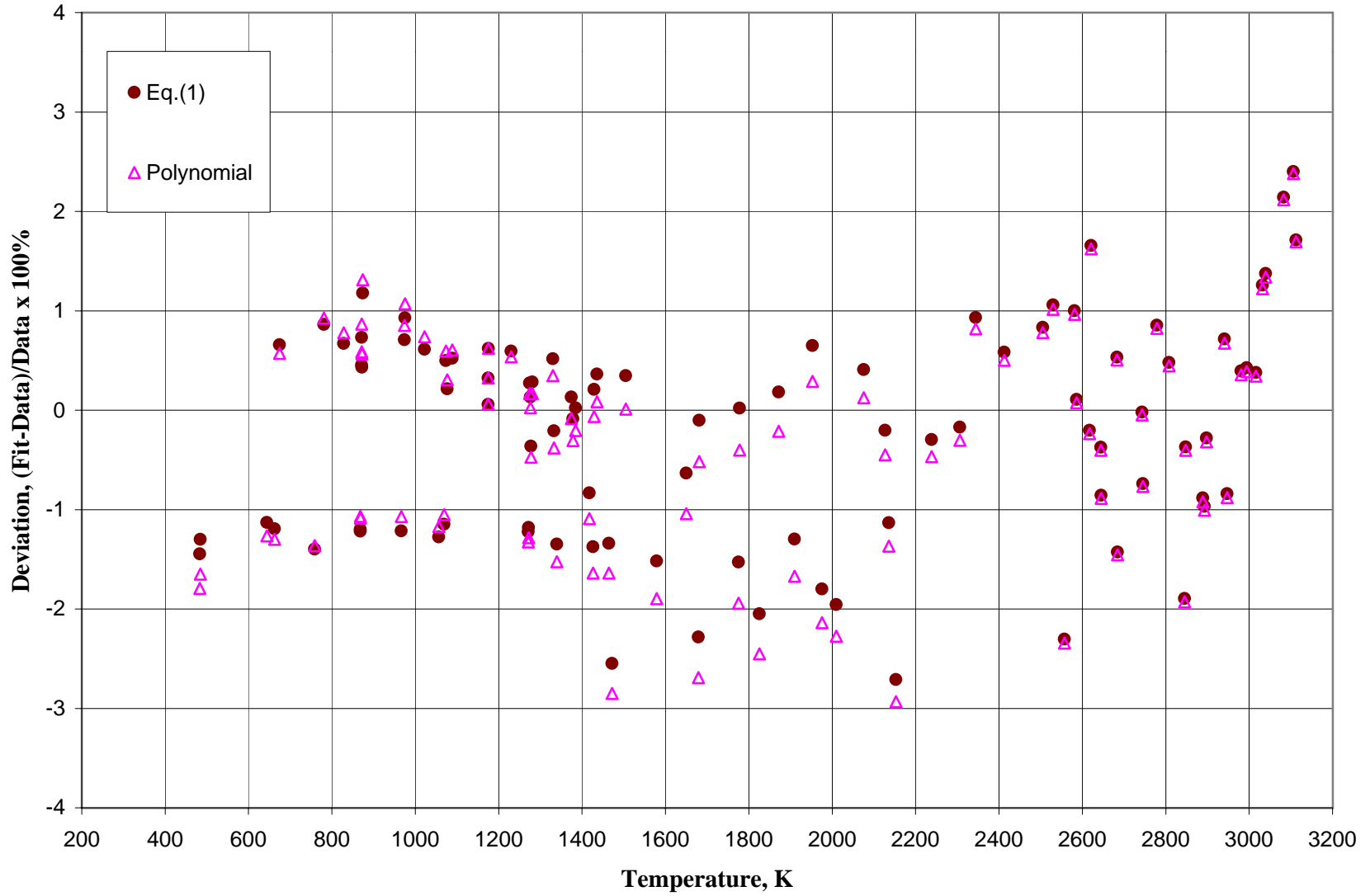
Figure 8 Percent Deviations of Enthalpy Data from the Recommended Equations

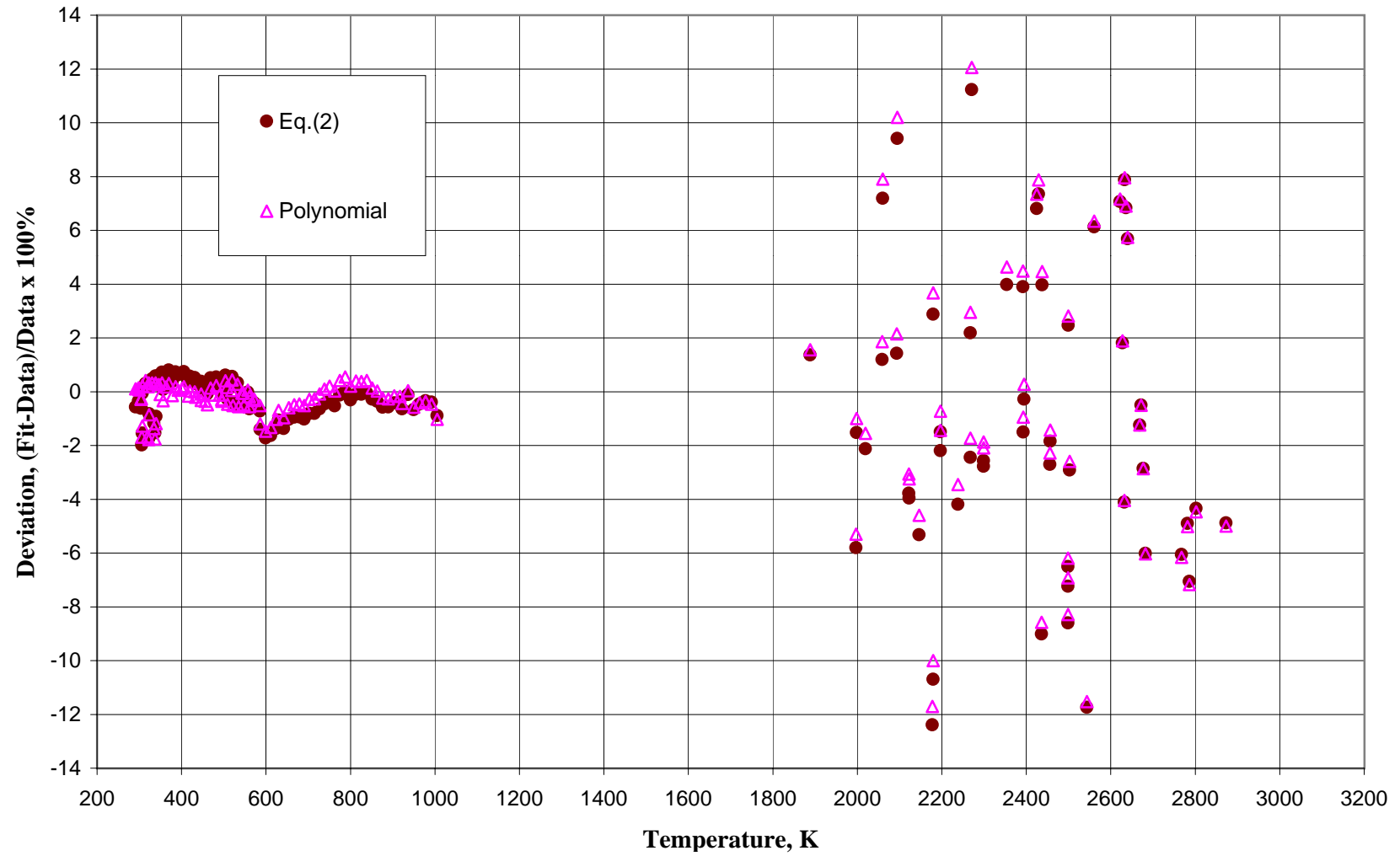
Figure 9 Percent Deviations of Heat Capacity Data from the Recommended Equations

Figure 10 Comparison of Recommended Equation & Data with MATPRO Equation